Eur. Phys. J. D **28**, 119–124 (2004)
DOI: 10.1140/epjd/e2003-00291-5

THE EUROPEAN PHYSICAL JOURNAL D

Stark broadening of hydrogen spectral lines with fine structure effects

W. Olchawa[a], R. Olchawa, and B. Grabowski

Institute of Physics, Opole University, Oleska 48, 45-052 Opole, Poland

Received 25 June 2003 / Received in final form 12 September 2003
Published online 21 October 2003 –

Abstract. Formalism and numerical code have been elaborated for calculation of hydrogen line profiles in conditions of plasma in which Stark broadening and fine energy splitting are comparable and it is not possible to neglect either of them. It corresponds to the range of electron densities $10^{11} < N_e\ (\mathrm{cm}^{-3}) < 10^{15}$. Lamb shift and spontaneous emission effects have also been included. Computer simulation method was applied in the calculations. Final results have been compared with experimental and theoretical findings by other authors.

PACS. 32.70.Jz Line shapes, widths, and shifts – 52.20.-j Elementary processes in plasmas

1 Introduction

Investigation of the Stark shapes of hydrogen spectral lines is one of the basic problems of the atomic plasma spectroscopy. The great interest in these problems results, among other things, from the existence of a possibility of using half-widths of these lines to simple, and non-invasive, determination of the electron concentration N_e in plasma. It is obvious that the more realistic the theoretical model of the line profile is, the more precise is this tool in the N_e measurements. In some applications, however, the knowledge of the half-width of the line profile alone is insufficient. For example, in the case of modeling of the synthetic stellar spectra, knowledge of the complete line profiles is necessary. In such a type of applications, the data bases of the theoretical line profile calculations are especially useful, when the results are presented in the tabular form. In the past the tables of the hydrogen line profiles published by Griem [1] (being the numerical result of the approach proposed in papers by Kepple and Griem [2], or by Vidal et al. [3]) were commonly used. The numerical values of the line half-widths placed there are considerably smaller than the measured ones (see Fig. 6). This discrepancy increases when the electron concentration N_e in plasma decreases. The main cause of this discrepancy is neglecting the thermic motion of ions, i.e. carrying out the calculations within the quasi-static approximation for ions. A considerably better (compared with the quasi-static results) agreement of the calculated and measured hydrogen line profiles is given by the method of model microfields (MMM) approximation, e.g. [4]. The Stark line profiles (calculated within this approximation), and the convolutions of these profiles with proper Doppler broadening, are published in a tabular form by Stehle [5], Stehle and Hutcheon [6], and also — in its enlarged version — on the Internet page `dasgal.obspm.fr/~stehle`. In papers: Gigosos and Cadenoso [7]; Alexiou et al. [8], and Sorge and Günter [9], it is shown that the numerical values of the line half-widths, obtained within the MMM approximation are, however, still smaller than the measured ones. A particularly clear discrepancy appears in the case of lines with a strong central component, as e.g. Ly_α and H_α. In the paper by Sorge and Günter [9], it is shown particularly that the simulated autocorrelation function for the ionic microfield differs significantly from the autocorrelation function applied within the MMM approach. This discrepancy seems to point out that the usage of the Markoff-process formalism within the MMM approach describing the local microfield fluctuations in plasma is rather unfounded. The line profile calculated to-day, using the so-called full computer simulation method (FCSM) [7], agrees with the measurements in the best way. The extensive tabular data on the Stark full-widths at half maximum (FWHM), calculated thereby, were published in [7]. These results agree very well with the experimental data above some (specific of each individual spectral line) limiting electron concentration N_e in plasma. For example, for H_α line the limiting N_e value amounts to about $10^{15}\ \mathrm{cm}^{-3}$. Below this limit an increasing discrepancy between the theory and measurements appears. In all the above-mentioned calculations the cause of the appearing discrepancy is neglecting the contribution of the fine structure effect in formation of the spectral line shapes. Pastor et al. [10], took a step forward, i.e. calculated, via FCSM, the Stark line profile of H_α line, taking into account the fine structure effect. We would like to point out, however, that the Stark line profile

[a] e-mail: `wolch@uni.opole.pl`

calculations, taking into consideration the fine structure effect (but using the simplifying impact approximation for ions) were carried out for the first time by Stehle and Feathier [11]. These last calculations agree fairly well with measurements at very low electron concentrations only, i.e. at $N_e < 10^{13}$ cm^{-3}. Within the calculations by Pastor et al. [10], and Stehle and Feautrier [11], the contribution of the Doppler effect was neglected. This delimits the possibility of the experimental testing and of the diagnostic applicability of these results. The experimental checking can be done by methods of the free-Doppler spectroscopy only. Moreover, these results are useful to describe the line profiles in plasma spectra (when the Doppler effect is not negligible) only with the additional, simplifying assumption that the Stark and Doppler effects are independent. (Such a simplification is made when the Stark-Doppler convolution is calculated.) Within the range of the middle electron concentrations (10^{13} cm^{-3} $< N_e <$ 10^{15} cm^{-3}), where both Stark and Doppler mechanisms are comparable, we expect that taking into account the correlations of these both effects can be necessary and quantitatively significant. The aim of the present paper is to build such a numerical code of the hydrogen line profile calculations, within the framework of which the FCSM approach could simultaneously take into account the following effects of:

(i) the fine structure,
(ii) the Stark-Doppler coupling,
(iii) the natural width of the line.

A simultaneous taking of all these effects into account is important and necessary for plasmas of electron concentrations 10^{11} cm^{-3} $< N_e <$ 10^{16} cm^{-3}. This N_e range is principally significant for an interpretation of all the normal stellar spectra.

2 Theoretical approach

The computer simulation method for computing the spectral line profiles was used for the first time by Seidel and Stamm [12]. The authors calculated the hydrogen line profile of: Ly$_\alpha$, Ly$_\beta$, and Ly$_\gamma$, taking the Stark and Doppler broadening simultaneously into account. They carried out the calculations in two variants, i.e. within the so-called:

(i) exact model,
(ii) μ-ion model.

Within the approach (i) the coupling between the Stark and Doppler broadening is taken into account. In the case (i), and in the co-ordinate system connected with a statistical emitter, the plasma is non-isotropic. In the approach (ii) — the plasma is isotropic, and the Stark profile is convoluted with the Doppler profile. However, approach (ii) demands a simplifying assumption that the Stark and Doppler broadening mechanisms are statistically independent one of another. With this simplification, when calculating the Stark line profile, the ion mass is replaced by the "effective" mass μ, equal to the reduced mass of the emitter-perturbing ion pair. In the case when the Stark broadening considerably predominates over the Doppler broadening, the μ-ion model gives correct results [7,12–14]. Exact calculations have been carried out also in the frame of the so-called collision time statistics. Kesting [13] demonstrated that the exact calculations are well reproduced by the so-called μ^*-ion model. The predominance of the μ^*-ion model over the exact model [13] lies in the fact that the μ^*-ion model allows — using the co-ordinate system attached to a statistical emitter — treating the plasma as an isotropic medium and, simultaneously, the coupling between the Stark and Doppler broadening is, at least approximately, included. This property is very useful in plasma simulation, which will be exploited in Section 3 of the present paper. In the μ^*-ion model, in the reference frame attached to the emitter, the emitter stays at rest and interacts with fictitious ions, to which the mass μ^* is attributed, according to the following relations [13]:

$$\mu^*(u) = \frac{m}{g^2(\frac{u}{v_0})}, \tag{1}$$

and

$$g(x) = \frac{1}{2}\exp(-x^2) + \frac{\sqrt{\pi}}{4}(1+2x^2)\frac{\mathrm{erf}(x)}{x}, \tag{2}$$

where m is true ion mass, u is the emitter speed in the laboratory reference frame, and $v_0 = \sqrt{2kT/m}$. Within the classical path approximation and the spontaneous dipole transition, the line profile formula is as follows:

$$I(\omega) = \frac{1}{\pi}\mathrm{Re}\int_0^\infty e^{i\omega t}C(t)dt, \tag{3}$$

where $C(t)$ is the dipole autocorrelation function. In the μ^*-ion model the function is as follows:

$$C^{(\mu^*)}(t) = N\ \mathrm{Tr}\left\{\mathbf{d}(0)\left\langle\frac{\sin(\omega_0 utc)}{\omega_0 utc}\mathbf{d}(t)\right\rangle_{u,p}\right\}, \tag{4}$$

$$N = \mathrm{Tr}\{\mathbf{d}(0)\mathbf{d}\}^{-1}, \tag{5}$$

where $\mathbf{d}(0)$ and $\mathbf{d}(t) = U^{-1}\mathbf{d}(0)U$ are the dipole momentum operators of the emitter, U is the time development operator, ω_0 is the unperturbed frequency of the radiation of the transition, at the centre of gravity of the multiplet, c is the light speed, and symbol $\langle\ldots\rangle_{u,p}$ indicates the averaging over the emitter velocities and the initial configurations of ions and electrons. If plasma-emitter interactions are limited to the dipole approximation, the time development operator U will obey the following form of the Schrödinger equation:

$$i\hbar\dot{U} = (H - \mathbf{d}\cdot\mathbf{F}(t))U, \tag{6}$$

where H is the Hamiltonian of the isolated emitter,

$$H = H_0 + H_{FS} + H_{LR} - i\Gamma \tag{7}$$

consisting of: the fine structure (e.g. [7])

$$H_{FS} = -\frac{p^4}{8m_0^3c^2} + \frac{Ze^2}{2m_0^2c^2}\frac{1}{r^3}\mathbf{L}\cdot\mathbf{S} + \frac{\pi\hbar^2Ze^2}{2m_0^2c^2}\delta(\mathbf{r}), \tag{8}$$

the Lamb shift H_{LR}, and the natural width of the energy level Γ. Symbol $\mathbf{F}(t)$ represents the uniform electrical field produced by ions and electrons at the position of a given emitter. The remaining symbols have the conventional meanings. The Pauli functions have been used as basis to solve the Schrödinger equation, defined by equation (6):

$$\Psi_{nljm_j} = \frac{1}{\sqrt{2l+1}} R_{nl}(r) \times \begin{pmatrix} \pm\sqrt{l \pm m_j + 1/2}\, Y_{l,m_j-1/2}(\theta,\phi) \\ \sqrt{l \mp m_j + 1/2}\, Y_{l,m_j+1/2}(\theta,\phi) \end{pmatrix} \quad \text{for} \quad j = l \pm 1/2, \quad (9)$$

being the solution of the timeless Schrödinger equation

$$(H_0 + H_{FS})\Psi = E_{nj}\Psi, \quad (10)$$

where

$$E_{nj} = -\mathrm{Ry}\left(\frac{Z}{n}\right)^2 - \alpha^2 \mathrm{Ry}\left(\frac{Z}{n}\right)^4 \left[\frac{n}{j+1/2} - \frac{3}{4}\right]. \quad (11)$$

Finally, the eigenvalue of the isolated hydrogen atom in the state $|n,l,j,m\rangle$, can be written as follows:

$$E_{nljm_j} = E_{nj} + \Delta E_{nl} - i\Gamma, \quad (12)$$

where ΔE_{nl} is the Lamb shift (we take that from Ref. [15]), and

$$\Gamma = \frac{\hbar}{2\tau_{nljm_j}}, \quad (13)$$

where τ_{nljm_j} — the lifetime of the emitter in the quantum state $|n,l,j,m\rangle$. Of course, the off-diagonal matrix elements of the H_{RL} and Γ operators are equal to zero.

When we assume that the emitter velocity in equation (4) equals zero, $u = 0$, then the autocorrelation function $C^{(\mu^*)}(t)$ reduces to the Stark autocorrelation function $C_S^{(\mu^*)}(t)$. Please notice that in this limit (important for Doppler free spectroscopy) u is still different from zero in equation (1), so now the emitter stays at rest in the laboratory reference frame, but it is perturbed by fictitious ions, whose mass is obtained from equation (1). The function obtained in this way differs from the Stark autocorrelation function $C_S^{(\mu)}(t)$ of the μ-ion model. This first function is formed under the perturbations by ions, the mass of which is defined in each individual initial configuration. In the μ-ion model, however, in all configurations the ion mass is the same, equal to the reduced mass of the ion-emitter pair. The autocorrelation function $C^{(\mu)}(t)$ of the μ-ion model can be calculated as a product of the autocorrelation function $C_S^{(\mu)}(t)$ and the Doppler autocorrelation function $C_D(t)$, i.e.:

$$C^{(\mu)}(t) = C_S^{(\mu)}(t) \times C_D(t), \quad (14)$$

where

$$C^{(\mu)}(t) = N\ \mathrm{Tr}\{\mathbf{d}(0) \cdot \langle \mathbf{d}(t) \rangle_p\}, \quad (15)$$

and

$$C_D(t) = \left\langle \exp\left(-i\omega_0 \frac{\mathbf{k}\cdot\mathbf{u}}{c} t\right) \right\rangle_p = \exp\left(-\frac{\omega_0^2 u_0^2}{4c^2} t^2\right), \quad (16)$$

where $u_o = \sqrt{2kT/M}$, and M is the emitter mass.

3 The full computer simulation method

In the frame of the above-mentioned μ^*-ion model we performed calculations of Ly_α, Ly_β, $\mathrm{H}\alpha$, H_β, H_γ, and P_α line shapes using our own method — FCSM. The applied method is described in detail in paper [16] and in the Ph.D. thesis by Olchawa [17]. Some additional comments concerning the FCSM may also be found in reference [18]. Therefore, below only a short description of FCSM is given. Because within the μ^*-ion model the plasma is isotropic, we accepted that the statistical emitter interacts only with perturbers (electrons and ions) occurring within the sphere of the radius of $R_{\max} = 3D$ (D — the Debye electronic radius). In the centre of the sphere a stiff ball (with the radius of $R_{\min} = (3/2)a_0 n_i^2$) is placed, which represents the emitter, the perturbers are reflected at this ball according to the classical reflection law. (The symbol a_0 is the Bohr radius, n_i — the principal quantum number of the upper energetic level of the transition.) The electron and ions (the latter of mass μ^*) are moving along straight trajectories, with velocities generated (random sampling) according to the Maxwell distribution. A perturber escaping the defined plasma volume is replaced by "new" perturber of the same velocity value as that of the escaping one, but with a random spatial orientation. The number of the initial configurations of the perturbers amounted to 500–1000. The Schrödinger equation, equation (6), has been solved using the Fehlenberg adaptive stepsize method. The calculations have been carried out within the non-quenching approximation. Because the aim of the present paper is to examine subtle effects, checking the numerical noise is of substantial importance. To this end the calculations were done in two variants — but in the same physical conditions — using: (i) the complete Hamiltonian H given by equation (7), and (ii) the Hamiltonian H_0 in which all subtle effects are omitted. In references [19,20] it is shown that in the second case the imaginary part of the autocorrelation function equals zero, $\mathrm{Im}[C^{(\mu^*)}(t)] = 0$. Thus, the numerical deviation of $\mathrm{Im}[C^{(\mu^*)}(t)]$ from zero is a measure of the numerical noise within our calculations. In Figure 1 the autocorrelation functions, corresponding to both above variants, are presented as examples. Comparing the curves in Figure 1 we can see that in the relevant physical conditions of plasma the effects, investigated in the present paper (i.e. the fine structure effect — the leading effect amongst the examined ones, the Lamb shift, and the natural broadening), substantially contribute to the formation of the autocorrelation function of H_α line. At the same time, comparing

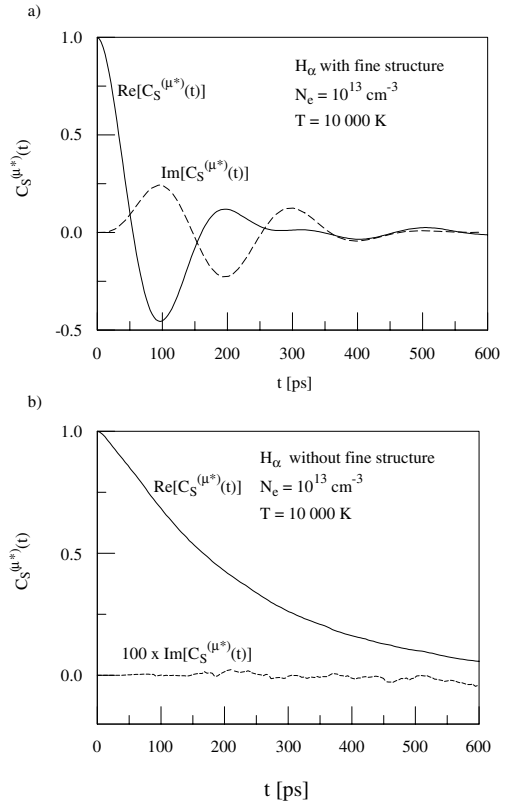

Fig. 1. The real and imaginary parts of the Stark autocorrelation function of the H_α line, calculated in the μ^*-ion model: (a) taking into account the fine structure, the Lamb shift, and the natural splitting, and (b) neglecting these effects. The calculations have been performed for the following physical conditions of plasma: $T = 10$ kK, $N_e = 10^{13}$ cm^{-3}.

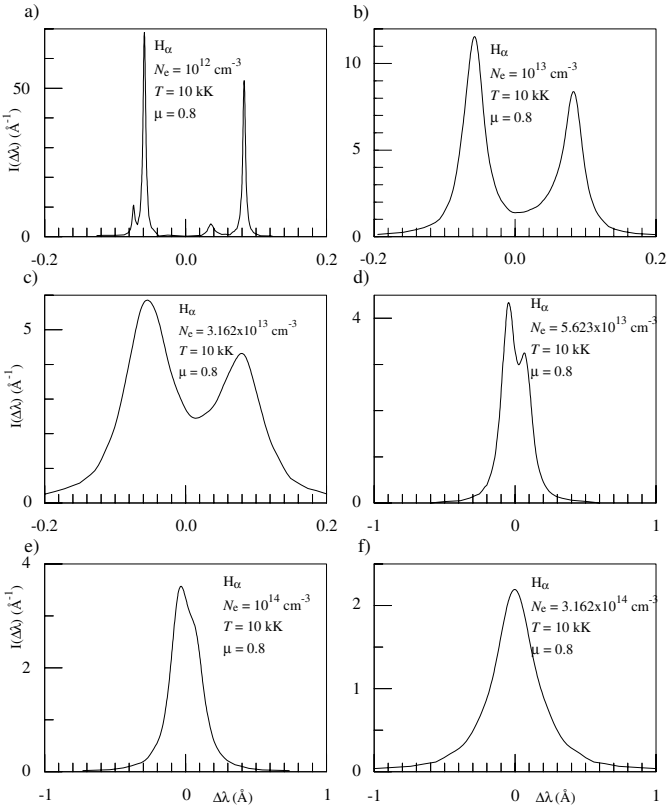

Fig. 2. The evolution of the calculated (without contribution of Doppler effect) H_α line shape changing the electron concentration N_e.

the imaginary parts of the autocorrelation functions, we see that the level of the numerical and statistical noise is smaller at least by two orders of magnitude than the numerical values of the calculated functions. So, our numerical code FCMS of the line shape calculations is perfectly able to take very subtle contributions into account, and, therefore, may be confidently used for investigating the effect being the subject of interest in the present paper.

4 Results and conclusions

Within the theoretical model, formulated in the present paper, we carried out the line profile calculations for Ly_α, Ly_β, H_α, H_β, H_γ, and P_α in the range of the following electron concentration 10^{11} cm$^{-3} < N_e < 10^{17}$ cm^{-3}. For the graphical presentation the H_α line was chosen as an example. We chose this example because of two reasons: firstly — the fine splitting (FS) of the H_α line is the greatest and, secondly — for this line the experimental data in the physical conditions in which FS has substantial importance, are accessible in the literature on the subject.

In Figure 2 an evolution of the H_α line shape, calculated within the μ^*-ion model, is shown as a function of the physical conditions of plasma. In these calculations the contributions due to the Stark broadening, the natural broadening, and the Lamb effect have been taken into account, whereas the Doppler effect has been omitted. We can see that when N_e diminishes, the line shape changes in such a way that FS becomes more and more visible. Often line width is defined in a different way for the case when the fine structure components are visibly separated and for the case when they overlap. We have used the following rule: comparing our line widths with experimental ones, for determining numerical value of line width, we apply the same parameter as that defined in the experiment under consideration. In reference [21] the numerical values of the line widths of H_α, measured using the Doppler free technique, are collected. In the physical conditions of plasma in the experiment [21] the line profiles have shapes similar to that in Figure 2b, i.e. strongly marked two FS components. In paper [21] two Lorentz profiles were matched to such a two-peak shape, assuming the same half-widths w of both line components; the value of w is understood as half-width of the H_α line profile. In case of the measurements [22] (Stark and Doppler) the typical definition — the full width at half maximum (FWHM) — was used. In Figure 3 the numerical values of the line widths of H_α: the ones calculated by us and those measured, are compared. Our theoretical results agree very well with the measurements by Ehrich and Kelleher [22]. Comparing these with the data of the experiment [1] we see a discrepancy of 25%.

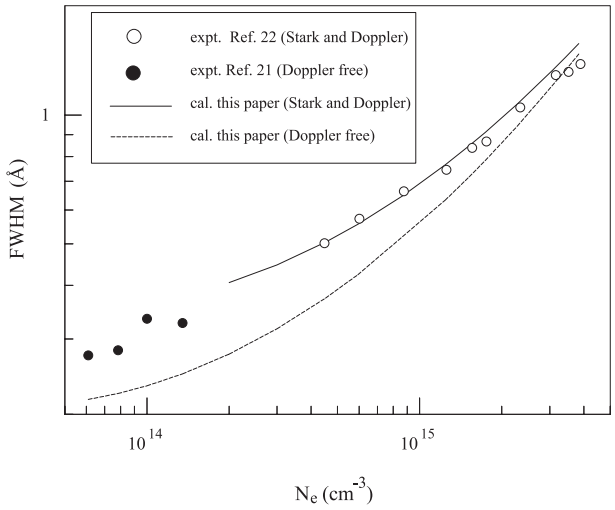

Fig. 3. Comparison of the calculated and measured line widths of H_α. The marks represent particular measurements: the full circles Weber et al. [21], the open circles Ehrich and Kelleher [22]. The lines represent our theoretical results.

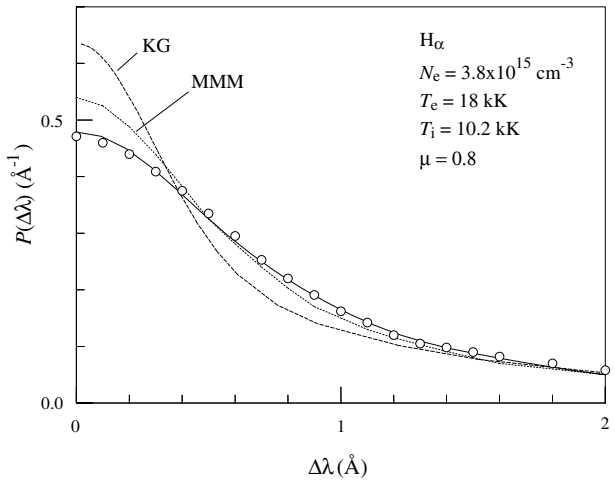

Fig. 4. Comparison of the calculated and measured line profiles of H_α. The open circles the measurements by Ehrich and Kelleher [22]; the lines represent the calculations: the dotted line Stehle [5], the dashed line corrected Kepple and Griem results, the solid line our results.

This discrepancy is still contained within limits of the experimental errors, given by the authors of reference [22].

Figure 4 presents, as an example, a comparison of the H_α line profiles: the measured one [22] and that calculated in the present paper, as well as calculated in other papers accessible in the literature of the subject. As we see, the agreement of our calculations with the measurements is excellent. We would like to point out that in the quasi-static approximation for ions performed by Kepple and Griem, in which the results (from Fig. 4 and subsequent ones) were obtained, the so-called interference term in the impact operator for ions has been corrected. After this correction, the results [3] (quasi-static approximation for ions and unified theory for electrons) almost adjust themselves to the corrected results of the type of Kepple and Griem.

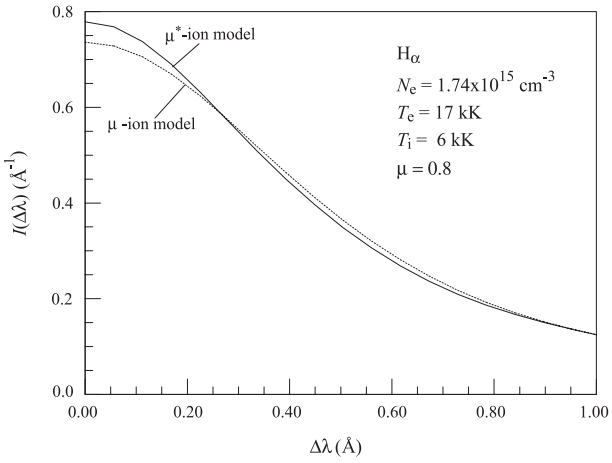

Fig. 5. Comparison of the line profiles of H_α, calculated within the present paper: the solid line μ^*-ion model, the dashed line μ-ion model.

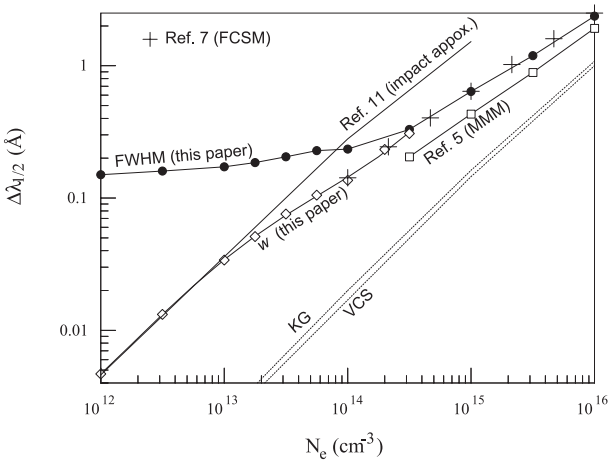

Fig. 6. Comparison of the calculated (without Doppler contribution) half widths of H_α line, as functions of the electron concentration N_e.

In order to estimate the importance of the Stark-Doppler coupling effect, in Figure 5 we compare the line profiles of the H_α, calculated within the μ^*-ion model (Stark-Doppler coupling) and the μ-ion model (Stark-Doppler convolution). The coupling effect strongly influences the line shape in its central part only; at the same time it changes the FWHM value insignificantly (at the most by 5%).

A comparison of the line widths of H_α (without Doppler contribution) calculated in the present paper and the ones calculated by other authors, is presented in Figure 6. We point out that at $N_e < 10^{13}$ cm^{-3} our results pass smoothly into the results obtained by Stehle and Feautrier [11] within the impact approximation for ions. Similarly, at $N_e > 5 \times 10^{14}$ cm^{-3} our results pass smoothly into FCSM results obtained by Gigosos and Cardenoso [7]. This means that our theoretical model (as well as our numerical code) works excellently, irrespective

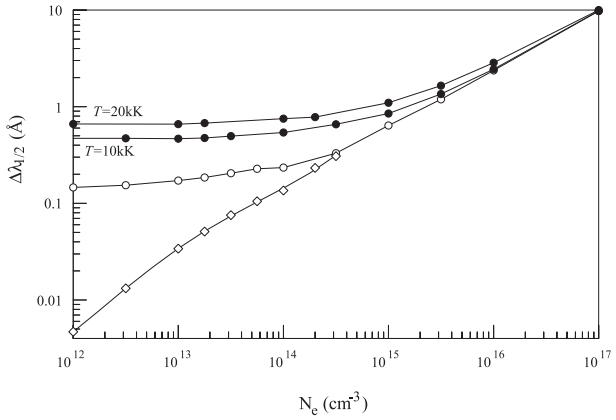

Fig. 7. Comparison of the half widths of the line profiles of H_α, calculated within the present paper alternatively: with (full marks) and without (open marks) Doppler contribution, as the functions of the electron concentration N_e. The diamonds represent w parameter according to definition from [21].

Table 1. Distinctive values of the electron concentration of N_e, defining regions of validity of the line-broadening mechanisms in plasmas, for initial lines in Lyman, Balmer and Paschen series. In first column are given the values of N_e, below which the so-called impact approximation acts satisfactorily. In second column are given the values of N_e, above which the fine structure (FS) of the line can be neglected. In third column are given the value of N_e, below which the Doppler effect at the temperature of gases 10 kK is predominating.

line	electron density N_e (cm^{-3})		
Ly_α	10^{14}	2×10^{15}	10^{16}
Ly_β	10^{13}	5×10^{13}	10^{15}
H_α	10^{13}	6×10^{14}	10^{15}
H_β	2×10^{12}	4×10^{13}	5×10^{14}
H_γ	3×10^{12}	10^{13}	5×10^{13}
P_α	3×10^{11}	2×10^{12}	10^{14}

of the electron concentration N_e in plasma. On the basis of Figure 6 we conclude that at $N_e < 5 \times 10^{14}$ cm^{-3} the contribution of FS to the line width of H_α must be taken into account. We point out also that the FWHM values resulting from MMM approach are slightly, but systematically, smaller than the results obtained by us and in reference [7]. It seems that this discrepancy results from differences between the fluctuations of the ionic microfield in real plasma and those assumed within the stochastic model, respectively. Finally, the reason for the observed great discrepancy between the results of our code and the approximations by KG and VCS (Refs. [2,3]) is complete omission of the ion dynamics within KG and VCS approaches.

The H_α line widths, calculated in the present paper with and without Doppler contribution, are compared in Figure 7. We see particularly that in the case of the H_α line emitted by plasmas in the physical conditions: $T = 10$ kK and $N_e < 10^{14}$ cm^{-3}, the Doppler effect is the predominant one. Furthermore, one can define a lower limit, $N_e \approx 10^{15}$ cm^{-3}, above which the methods of N_e determination from the line-width measurements may be used confidently. An analogous (as in Figs. 6 and 7) analysis of the obtained results has been carried out for the spectral lines: Ly_α, Ly_β, H_β, H_γ, and P_α. The numerical results of that analysis are gathered in Table 1.

References

1. H.R. Griem, *Spectral Line Broadening by Plasmas* (Academic Press, New York, 1974)
2. P. Kepple, H.R. Griem, Phys. Rev. **173**, 317 (1968)
3. C.R. Vidal, J. Cooper, E.W. Smith, Astrophys. J. Suppl. **25**, 37 (1973)
4. J. Seidel, Z. Naturforsch. **32a**, 1195 (1977)
5. C. Stehle, Astron. Astrophys. Suppl. Ser. **104**, 509 (1994)
6. C. Stehle, R. Hutcheon, Astron. Astrophys. Suppl. Ser. **140**, 93 (1999)
7. M.A. Gigosos, V. Cardenoso, Phys. Rev. A **37**, 5258 (1989); J. Phys. B: At. Mol. Phys. **29**, 4795 (1996)
8. S. Alexiou, P. Poquerusse, E. Leboucher-Dalimier, Phys. Rev. E **59**, 3499 (1999)
9. S. Sorge, S. Günter, Eur. Phys. J. D **12**, 369 (2000)
10. R. Pastor, M.A. Gigosos, M.A. Gonzalez, in *Spectral Line Shapes*, edited by J. Seidel (API, Berlin, 2000), Vol. 11, p. 79
11. C. Stehle, N. Feauteier, J. Phys. B: At. Mol. Phys. **18**, 1297 (1985)
12. J. Seidel, R. Stamm, J. Quant. Spectrosc. Radiat. Transf. **27**, 499 (1982)
13. G.C. Hegerfeld, V. Kesting, Phys. Rev. A **37**, 1488 (1988); V. Kesting, Ph.D. thesis, Georg-August-Universität, Göttingen, 1992
14. R. Stamm, E.W. Smith, Phys. Rev. A **30**, 2039 (1984)
15. H.A. Bethe, E.E. Salpeter, *Quantum mechanics of one- and two-electron atoms* (Springer-Verlag, Heidelberg, 1957)
16. J. Halenka, W. Olchawa, J. Quant. Spectrosc. Radiat. Transf. **56**, 17 (1996)
17. W. Olchawa, Ph.D. thesis, Nicholas Copernicus University, Torun, 1997
18. T. Wujec, W. Olchawa, J. Halenka, J. Musielok, Phys. Rev. E **66**, 066403 (2002)
19. J. Halenka, Phys. Rev. E (2003, accepted)
20. S. Alexiou, J. Quant. Spectrosc. Radiat. Transf. **81**, 13 (2003)
21. E.W. Weber, R. Frankenberg, M. Schiling, Appl. Phys. B **32**, 63 (1983)
22. H. Ehrich, D.E. Kelleher, Phys. Rev. A **21**, 319 (1980)